MATERIALS PHYSICS AND MECHANICS RESEACH ARTICLE

Submitted: June 13, 2023 **Revised: October 31, 2023** **Accepted: March 25, 2024**

Variants of physical equations in a curvilinear coordinate system and their comparison based on mixed FEM

R.Z. Kiseleva [1]✉, N.A. Kirsanova [2], A.P. Nikolaev [1], Yu.V. Klochkov [1], V.N. Yushkin [1]

[1] Volgograd State Agrarian University, Volgograd, Russia

[2] Financial University under the Government of the Russian Federation, Moscow, Russia

✉ rumia1970@yandex.ru

ABSTRACT

In arbitrary curvilinear coordinate system under elastoplastic deformation, a comparative analysis of three variants of the constitutive equations at the loading step was performed. In the first variant, the equations of the theory of plastic flow were used, according to which the strain increment had been divided into elastic and plastic parts. The cumbersomeness of the algorithm for obtaining expressions for the components of the plastic strain increments tensor in an arbitrary curvilinear coordinate system is shown, which leads to the lack of the possibility of obtaining the matrix dependence of physical equations at the loading step. In the second variant, to obtain plastic strain increments, the hypothesis of their proportional dependence on the components of the stress increments deviator was used. The constitutive equations were also obtained by summation of the elastic strains increment and plastic strains increment. In the third variant, the hypothesis of the division of strain increments into elastic and plastic parts was not used. The physical equations were written using the assumption that there was a proportional dependence between the components of the strain increment deviators and stress increment deviators. Using the example of calculating the shell of revolution, the preference of the third variant of the constitutive equations for elastoplastic deformation is shown.

KEYWORDS

shell of revolution • physical nonlinearity • hexahedral finite element • mixed functional • mixed FEM implementation

Acknowledgements. *This work was performed within the State assignment of Federal Scientific Research Center "Crystallography and Photonics" of Russian Academy of Sciences.*

Citation: Kiseleva RZ, Kirsanova NA, Nikolaev AP, Klochkov YuV, Yushkin VN. Variants of physical equations in a curvilinear coordinate system and their comparison based on mixed FEM. *Materials Physics and Mechanics*. 2024;52(3): 33–43.
http://dx.doi.org/10.18149/MPM.5232024_4

Introduction

When calculating structures taking into account elastoplastic deformations, it is necessary to take into account the behavior of the material, including the formation of residual deformations. Determining the values of the stress-strain state during deformation beyond the elastic limit makes it possible to establish the maximum load and assign a safety factor. Therefore, calculations of structural elements taking into account zones of elastoplastic deformation are an urgent engineering problem for mechanical engineering, aircraft structures, hydraulic structures, etc. Currently, the most used theories for finding the strength parameters of deformed objects are the deformation theory of plasticity and the theory of plastic flow [1–15]. Numerical implementation of the defining equations of the theories of plasticity is widely carried out using the finite element method (FEM) in the

Publisher: Peter the Great St. Petersburg Polytechnic University

displacement method formulation [16–23] and in the mixed formulation [22,24–30]. Widely used theories of plasticity (the theory of small elastoplastic deformations and the theory of plastic flow) use the hypothesis of dividing strain increments into elastic and plastic parts. In the theory of plastic flow, for the components of the plastic strain increment tensor are determined based on the assumption of their proportionality to the components of the total stress deviator with the coefficient of proportionality, which is a function of the stress intensity increment. To obtain physical equations at the loading step, it is necessary to represent the stress intensity increment through the increments of the components of the stress increment tensor, which is very difficult in a curvilinear coordinate system. The authors considered three variants of defining equations as physical ratios. In the first variant, equations of the theory of plastic flow were used. In the second variant, defining relations were used based on the assumption proposed by the authors about the proportional relation between the components of the plastic strain increments tensor and the components of the stress increments deviator. In the third variant, the defining equations were obtained without dividing the strain increments into elastic and plastic parts. The proportionality assumption was applied directly to the strain increments and stress increments deviator components. The coefficient of proportionality turned out to be a function of the tangent modulus of the strain diagram. For the numerical implementation of the equations, mentioned above, a hybrid finite element developed by the authors with nodal unknowns in the form of displacement increments and stress increments was used.

Materials and Methods

Relations of the theory of plastic flow

According to this theory, strain increments at the loading step consist of elastic strain increments $\Delta\varepsilon_{ij}^{e}$ and plastic strain increments $\Delta\varepsilon_{ij}^{p}$:

$$\Delta\varepsilon_{ij} = \Delta\varepsilon_{ij}^{e} + \Delta\varepsilon_{ij}^{p}. \quad (1)$$

Elastic strain increments are determined by Hooke's law [5–7]:

$$\Delta\varepsilon_{ij}^{e} = \frac{1}{2\mu}\Delta\sigma_{ij} - \frac{\lambda}{2\mu}g_{ij}\frac{1-2\nu}{E}P_{\Delta\sigma}; \quad (i,j = 1,2,3), \quad (2)$$

where λ, μ are the Lamé parameters, ν is the Poisson's ratio, $\Delta\sigma_{ij}$ are normal and tangential stresses increments, g_{ij} are the covariant components of the metric tensor at the loading step, E is the elastic modulus, $P_{\Delta\sigma} = \Delta\sigma_{mn}g^{mn} = \Delta\sigma^{mn}g_{mn}$ is the first invariant of the stress increments tensor.

The components of the plastic strain increments tensor in the theory of flow are determined [1] based on the hypothesis of a proportional relation between the components of the plastic strain increments tensor and the components of the stress deviator:

$$\Delta\varepsilon_{ij}^{p} = \frac{3}{2}\frac{\Delta\varepsilon_{i}^{p}}{\sigma_{i}}\left(\sigma_{ij} - \frac{1}{3}g_{ij}P_{\sigma}\right), \quad (3)$$

where $\Delta\varepsilon_{i}^{p}$ is the increment of the plastic strain intensity, σ_{i} is the stress intensity; $P_{\sigma} = \sigma_{ij}g^{ij} = \sigma^{ij}g_{ij}$.

The value of the intensity of plastic strain increments included in Eq. (3) is determined by the difference:

$$\Delta\varepsilon_i^p = \Delta\varepsilon_i - \Delta\varepsilon_i^e = \frac{\Delta\sigma_i}{E_k} - \frac{\Delta\sigma_i}{E_1}, \quad (4)$$

where $\Delta\varepsilon_i^p$, $\Delta\sigma_i$ are the increments of the intensities of plastic strain and stress increments, E_1 is the modulus of the initial section of the strain diagram, $E_к$ is the tangent modulus at the considered point of the strain diagram.

Relations (3) taking into account Eq. (4) are written as:

$$\Delta\varepsilon_{ij}^p = \Delta\sigma_i \frac{1}{\sigma_i}\left(\frac{1}{E_k} - \frac{1}{E_1}\right)\left(\sigma_{ij} - \frac{1}{3}g_{ij}P_\sigma\right). \quad (5)$$

To obtain relations between the values $\Delta\varepsilon_{ij}^p$ and $\Delta\sigma_{ij}$ the value $\Delta\sigma_i$ should be presented generally like:

$$\Delta\sigma_i = \frac{\partial\sigma_i}{\partial\sigma_{kl}}\Delta\sigma_{kl}, \quad (6)$$

where the stress intensity is determined in a curvilinear coordinate system by the expression [5]:

$$\sigma_i = \sqrt{\frac{3}{2}S^{ij}S_{ij}}. \quad (7)$$

The components of the stress deviator included in Eq. (7) are determined by the following formulas [5]:

$$S_{ij} = \sigma_{ij} - \frac{1}{3}g_{ij}\sigma_{mn}g^{mn}; \quad S^{ij} = g^{im}g^{in}S_{mn}. \quad (8)$$

Expression (6) taking into account Eq. (7) will take the form:

$$\Delta\sigma_i = \frac{\sqrt{3}}{2\sqrt{2}}\frac{1}{\sigma_i}\frac{\partial}{\partial\sigma_{kl}}\left(S^{ij}S_{ij}\right)\Delta\sigma_{kl}. \quad (9)$$

The plastic strain increments (5) taking into account Eq. (9) will be written as:

$$\Delta\varepsilon_{ij}^p = \gamma_1\frac{\partial}{\partial\sigma_{kl}}\left(S^{ij}S_{ij}\right)\Delta\sigma_{kl}, \quad (10)$$

where $\gamma_1 = \frac{\sqrt{3}}{2\sqrt{2}}\frac{1}{\sigma_i^2}\left(\frac{1}{E_к} - \frac{1}{E_1}\right)\left(\sigma_{ij} - \frac{1}{3}g_{ij}P_\sigma\right)$.

By summation of Eqs. (2) and (10), the matrix is formed:

$$\underset{6\times1}{\{\Delta\varepsilon\}} = \underset{6\times6}{\{C_1^{\Pi}\}}\underset{6\times1}{\{\Delta\sigma\}}, \quad (11)$$

where

$$\underset{1\times6}{\{\Delta\varepsilon\}}^{\mathrm{T}} = \{\Delta\varepsilon_{11}\ \Delta\varepsilon_{22}\ \Delta\varepsilon_{33}\ 2\Delta\varepsilon_{12}\ 2\Delta\varepsilon_{13}\ 2\Delta\varepsilon_{23}\ \};$$

$$\underset{1\times6}{\{\Delta\sigma\}}^{\mathrm{T}} = \{\Delta\sigma_{11}\ \Delta\sigma_{22}\ \Delta\sigma_{33}\ \Delta\sigma_{12}\ \Delta\sigma_{13}\ \Delta\sigma_{23}\ \}.$$

Due to the cumbersomeness of expressing the derivative in relation (9), the work on forming the matrix relation (11) in an arbitrary curvilinear coordinate system was not carried out in this research.

The second variant of plastic flow

It is proposed to determine the plastic strain increments based on the hypothesis of their proportionality to the components of the stress increments deviator [24]:

$$\Delta\varepsilon_{ij}^p = \frac{3}{2}\frac{\Delta\varepsilon_i^p}{\Delta\sigma_i}\left(\Delta\sigma_{ij} - \frac{1}{3}g_{ij}P_{\Delta\sigma}\right). \quad (12)$$

When taking Eq. (4) into account, Eq. (12) will be written in the form:

$$\Delta\varepsilon_{ij}^p = \frac{3}{2}\left(\frac{1}{E_к} - \frac{1}{E_1}\right)\left(\Delta\sigma_{ij} - \frac{1}{3}g_{ij}P_{\Delta\sigma}\right). \quad (13)$$

By summation of Eqs. (2) and (13), the relation is formed:

$$\Delta\varepsilon_{ij} = \left[\frac{1}{2\mu} + \frac{3}{2}\left(\frac{1}{E_к} - \frac{1}{E_1}\right)\right]\Delta\sigma_{ij} - g_{ij}P_{\Delta\sigma}\left[\frac{1}{2\mu}\frac{1-2\nu}{E} - \frac{1}{2}\left(\frac{1}{E_к} - \frac{1}{E_1}\right)\right], \quad (14)$$

as the matrix:

$$\underset{6\times1}{\{\Delta\varepsilon\}} = \underset{6\times6}{[C_2^{\Pi}]}\underset{6\times1}{\{\Delta\sigma\}}. \quad (15)$$

It should be noted that when obtaining the components of the plastic strain increment tensor, the hypothesis of the incompressibility of the material during plastic deformation was accepted.

The third variant of physical relations at the loading step

The relations between the stress and strain increments are obtained based on the assumption of a proportional relation between the components of the deviators of the stress and strain increments without dividing the increments of strain into elastic and plastic parts:

$$\Delta\varepsilon_{ij} - \frac{1}{3}g_{ij}P_{\Delta\varepsilon} = \frac{3}{2E_к}(\Delta\sigma_{ij} - \frac{1}{3}g_{ij}P_{\Delta\sigma}), \quad (16)$$

where $P_{\Delta\varepsilon} = \Delta\varepsilon_{mn}g^{mn}$ is the first invariant of the strain increments tensor.

The relation between the values of $P_{\Delta\varepsilon}$ and $\mathrm{P}_{\Delta\sigma}$ should be determined experimentally in the form of functional dependence $P_{\Delta\varepsilon} = \phi\mathrm{P}_{\Delta\sigma}$. It is assumed in this research that the relation between the first invariants of the strain increments tensors and stress increments in the process of elastic and plastic deformation remains unchanged:

$$P_{\Delta\varepsilon} = P_{\Delta\sigma}\frac{1-2\nu}{E}. \quad (17)$$

After substituting Eq. (17) into Eq. (16), the strain increments through the stress increments can be written in the form:

$$\Delta\varepsilon_{ij} = \frac{3}{2E_к}\Delta\sigma_{ij} - \psi g_{ij}\cdot P_{\Delta\sigma}, \quad (18)$$

where $\Psi = \frac{1}{2E_к} - \frac{1}{3}\ \frac{1-2\nu}{E}$.

Using Eq. (18), a matrix dependence is formed:

$$\underset{6\times1}{\{\Delta\varepsilon\}} = \underset{6\times6}{[C_3^{\Pi}]}\underset{6\times1}{\{\Delta\sigma\}}. \quad (19)$$

Shell geometry

The radius vector of an arbitrary point located at a distance *t* from the middle surface is written by the expression:

$$\boldsymbol{R}^{0t} = \boldsymbol{R}^0 + t\boldsymbol{a}^0, \quad (20)$$

where $\boldsymbol{R}^0 = x\boldsymbol{i} + r(x)\,sin\,\theta\,\boldsymbol{j} + r(x)\,cos\,\theta\,\boldsymbol{k}$ is the radius vector of the corresponding point of the middle surface of the shell of revolution, $\boldsymbol{a}^0$ is the normal to middle surface, *t* is the distance of a point from the middle surface.

At an arbitrary point, the basis vectors are determined by differentiation Eq. (20):

$$\boldsymbol{g}_m^0 = \boldsymbol{R}_{,m}^{0t} = \boldsymbol{R}_{,m}^0 + t\boldsymbol{a}^0. \quad (21)$$

The derivatives with respect to x, θ, t of the basis vectors of the point M^{0t} are determined by the components in the same basis [23]:

$$\underset{3\times1}{\{\boldsymbol{g}^0{}_{,x}\}} = \underset{3\times3}{[m]}\underset{3\times1}{\{\boldsymbol{g}^0\}};\quad \underset{3\times1}{\{\boldsymbol{g}^0{}_{,\theta}\}} = \underset{3\times3}{[n]}\underset{3\times1}{\{\boldsymbol{g}^0\}};\quad \underset{3\times1}{\{\boldsymbol{g}^0{}_{,t}\}} = \underset{3\times3}{[l]}\underset{3\times1}{\{\boldsymbol{g}^0\}}, \quad (22)$$

where $\underset{1\times3}{\{\boldsymbol{g}^0{}_{,\lambda}\}^T} = \{\boldsymbol{g}_1^0{}_{,\lambda}\,\boldsymbol{g}_2^0{}_{,\lambda}\,\boldsymbol{g}_3^0{}_{,\lambda}\};\quad \lambda = x, \theta, t.$

The displacement of the shell point M^{0t} at the loading step is determined by the vector:

$$\Delta\boldsymbol{V} = \Delta v^i\boldsymbol{g}_i^0. \quad (23)$$

Derivatives (23) of the vector will be written as:

$$\Delta \boldsymbol{V}_{,\lambda} = f_{\lambda}^{i}\boldsymbol{g}_{i}^{0}, \tag{24}$$

where

$$f_1^1 = \Delta v_{,x}^1 + \Delta v^1 m_{11} + \Delta v^2 m_{21} + \Delta v^3 m_{31}; \tag{25}$$
$$f_3^3 = \Delta v_{,t}^3 + \Delta v^1 l_{13} + \Delta v^2 l_{23} + \Delta v^3 l_{33}.$$

When the shell of rotation is deformed in a geometrically linear formulation, an arbitrary point M^{0t} will take the position M^t, determined by the radius vector:

$$\boldsymbol{R} = \boldsymbol{R}^{0t} + \Delta \boldsymbol{V}. \tag{26}$$

The basis vectors of the point M^t are determined by the differentiation Eq. (26):

$$\boldsymbol{g}_i = \boldsymbol{g}_i^0 + \Delta \boldsymbol{V}_{,i}. \tag{27}$$

The strain increments at the loading step are determined by the difference in the covariant components of the metric tensors [5]:

$$\Delta\varepsilon_{ij} = \frac{1}{2}(g_{ij} - g^0{}_{ij}) = \frac{1}{2}\left(\boldsymbol{g}_i^0 \cdot \Delta \boldsymbol{V}_{,j} + \boldsymbol{g}_j^0 \cdot \Delta \boldsymbol{V}_{,i}\right). \tag{28}$$

The strain increments $\Delta\varepsilon_{ij}$ taking into account Eqs. (24) and (25) could be presented through the vector components (23) in a matrix:

$$\underset{6\times1}{\{\Delta\varepsilon\}} = \underset{6\times3}{[L]}\,\underset{3\times1}{\{\Delta v\}}, \tag{29}$$

where $\underset{1\times3}{\{\Delta v\}^{\mathrm{T}}} = \{\Delta v^1\ \Delta v^2 \Delta v^3\}$ is the string of the displacement vector, $[L]$ is the matrix of differential and algebraic operators.

Strain matrix of the finite element at the loading step

A hexahedral finite element with eight nodal points $w = i, j, k, l, m, n, p, h$, the strain matrix of which is obtained in a mixed FEM formulation when choosing as nodal unknowns in the form of displacement increments and stress increments. The coordinates of the hexahedron through the coordinates of the nodes were determined by trilinear functions of local coordinates $\xi,\ \eta,\ \zeta$, varying within $-1 \le \xi,\ \eta\zeta \le 1$.

$$\lambda = \underset{1\times8}{\{f(\xi,\eta,\zeta)\}^T}\underset{8\times1}{\{\lambda_y\}}, \tag{30}$$

where λ is a global coordinate x, θ, t, $\underset{8\times1}{\{\lambda_y\}^{\mathrm{T}}}$ is the string of nodal coordinate values λ.

Displacement increments were also approximated using Eq. (30):

$$\underset{3\times1}{\{\Delta v\}} = \underset{3\times24}{[A]}\,\underset{24\times1}{\{\Delta v_y\}}, \tag{31}$$

where $\underset{1\times24}{\{\Delta v_y\}^T} = \{\Delta v^{1i} \ldots\ \Delta v^{1h}\Delta v^{2i} \ldots \Delta v^{2h}\Delta v^{3i} \ldots \Delta v^{3h}\}$ is the string of hexahedral nodal displacement.

Taking Eq. (31) into account, strains (29) will be written by the matrix expression:

$$\underset{6\times1}{\{\Delta\varepsilon\}} = \underset{6\times3}{[L]}\ \underset{3\times24}{[A]}\ \underset{24\times1}{\{\Delta v_y\}} = \underset{6\times24}{[B]}\ \underset{24\times1}{\{\Delta v_y\}}. \tag{32}$$

Stress increments in the vicinity of the internal point of the hexahedral are approximated by Eq. (30):

$$\Delta\sigma_{sr} = \underset{1\times8}{\{f(\xi,\eta,\zeta)\}^T}\underset{8\times1}{\{\Delta\sigma_{sr}^w\}}, \tag{33}$$

where $\underset{1\times8}{\{\Delta\sigma_{sr}^w\}^T} = \{\Delta\sigma_{sr}^i\Delta\sigma_{sr}^j\ \Delta\sigma_{sr}^k\ \Delta\sigma_{sr}^l\Delta\sigma_{sr}^m\ \Delta\sigma_{sr}^n\ \Delta\sigma_{sr}^p\Delta\sigma_{sr}^h\}$.

Using Eq. (33), the matrix relation is formed [8]:

$$\underset{6\times1}{\{\Delta\sigma_{sr}\}} = \underset{6\times48}{[S]}\,\underset{48\times1}{\{\Delta\sigma_y\}}, \quad (34)$$

where $\underset{1\times6}{\{\Delta\sigma_{sr}\}^T} = \{\Delta\sigma_{11}\Delta\sigma_{22}\Delta\sigma_{33}\Delta\sigma_{12}\Delta\sigma_{13}\Delta\sigma_{23}\};$

$$\underset{1\times48}{\{\Delta\sigma_y\}}^{\mathrm{T}} = \{\Delta\sigma_{11}^i\Delta\sigma_{11}^j\Delta\sigma_{11}^k\Delta\sigma_{11}^l\Delta\sigma_{11}^m\Delta\sigma_{11}^n\Delta\sigma_{11}^p.\Delta\sigma_{11}^h\ldots$$

$$\ldots\Delta\sigma_{23}^i\Delta\sigma_{23}^j\Delta\sigma_{23}^k\Delta\sigma_{23}^l\Delta\sigma_{23}^m\Delta\sigma_{23}^n\Delta\sigma\vdots{}^p_{23}\Delta\sigma_{23}^h\}.$$

To obtain the stress-strain state matrix at the loading step, a mixed functional was used [25]:

$$\Pi \equiv \int_V \underset{1\times6}{\{\Delta\sigma^{sr}\}^T}\underset{6\times3}{[L]}\underset{3\times1}{\{\Delta v\}}dV - \frac{1}{2}\int_V \underset{1\times6}{\{\Delta\sigma^{sr}\}^T}\underset{6\times6}{[C_{\kappa}^{\Pi}]}\underset{6\times1}{\{\Delta\sigma_{sr}\}}dV - \frac{1}{2}\int_S \underset{1\times3}{\{\Delta v\}^T}\underset{3\times1}{\{\Delta q\}}dS -$$

$$-\int_S \underset{1\times3}{\{\Delta v\}^T}\underset{3\times1}{\{q\}}dS + \int_V \underset{1\times6}{\{\sigma^{sr}\}^T}\underset{6\times1}{\{\Delta\varepsilon\}}dV; \quad (\kappa = 1,2,3). \quad (35)$$

Taking into account approximating Eqs. (31), (32) and (34), Eq. (35) will be written as:

$$\Pi \equiv \underset{1\times48}{\{\Delta\sigma_y\}^T}\int_V \underset{48\times6}{[S]}^T\underset{6\times6}{[G]^T}\underset{6\times24}{[B]}\,dV\underset{24\times1}{\{\Delta v_y\}} - \frac{1}{2}\underset{1\times48}{\{\Delta\sigma_y\}^T}\int_V \underset{48\times3}{[S]}^T\underset{6\times6}{[G]^T}\underset{6\times6}{[C_{\kappa}^{\Pi}]}\underset{6\times48}{[S]}\,dV\underset{48\times1}{\{\Delta\sigma_y\}} -$$

$$-\frac{1}{2}\underset{1\times24}{\{\Delta v_y\}^T}\int_S \underset{24\times3}{[A]}^T\underset{3\times1}{\{\Delta q\}}dS - \underset{1\times24}{\{\Delta v_y\}^T}\int_S \underset{24\times3}{[A]}^T\underset{3\times1}{\{q\}}dS + \underset{1\times24}{\{\Delta v_y\}^T}\int_V \underset{24\times6}{[B]}^T\underset{6\times1}{\{\sigma^{sr}\}}dV, \quad (36)$$

where the following relation is used $\underset{6\times1}{\{\Delta\sigma^{sr}\}} = \underset{6\times6}{[G]}\{\sigma_{sr}\}$.

By varying Eq. (36) according to the nodal unknowns, the stress-strain state matrix [*K*] is formed at the loading step [8]:

$$\underset{72\times72}{[K]}\,\underset{72\times1}{\{Z_y\}} = \underset{72\times1}{\{F_y\}}, \quad (37)$$

where $\underset{1\times72}{\{Z_y\}}^{\mathrm{T}} = \left\{\underset{1\times48}{\{\Delta\sigma_y\}^T}\,\underset{1\times24}{\{\Delta v_y\}^T}\right\}$ is the vector of finite element nodal unknowns;

$\underset{1\times72}{\{F_y\}}^{\mathrm{T}} = \left\{\underset{1\times48}{\{0\}^T} : \underset{1\times24}{\{\Delta f_q\}^T} + \underset{1\times24}{\{R\}^T}\right\}$ is the vector of nodal loads with residual $\{R\}^T$.

Using the developed strain matrix of a hexahedral finite element, it is possible to perform calculations during elastoplastic deformation with any hardening law, except for the horizontal section of the strain diagram ($E_k = 0$).

Results and Discussion

Example 1. The stress state of a shell of revolution with the middle surface of a truncated ellipsoid (Fig. 1) under the influence of internal pressure was considered. The following input data was used: a = 0.15 m; $в$ = 0.10 m; h = 0.01 m; l_k = 0.14 m; z_k = 0.0359 m; $E = 2\cdot10^5$ MPa; ν = 0.3.

When discretizing the shell, the bases of the hexahedral elements were located in the shell surfaces located at distances $t = t_1$ and $t = t_2$ from the middle surface. The edges of the elements accepted the normals to the middle surface.

The strain diagram was accepted with a section of nonlinear hardening (Fig. 2) with the following values of its characteristics: σ_{iT} = 200 MPa; $\varepsilon_{iT} = 0.866667\cdot10^{-3}$; ε_{ik} = 0.019; σ_{ik} = 400 MPa.

The function $\sigma_i = f(\varepsilon_i)$ is taken in the form of a parabola $\sigma_i = a_1\varepsilon_i^2 + b_1\varepsilon_i + c_1$ with numerical values of the constants: a = -6612835.5282 MPa; b = 242231.47902 MPa; c = 1795.0330258 MPa.

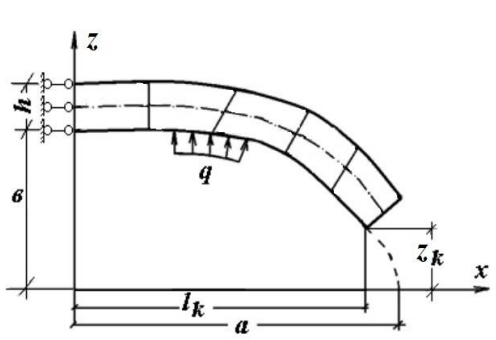

Fig. 1. Design diagram of a truncated ellipsoid

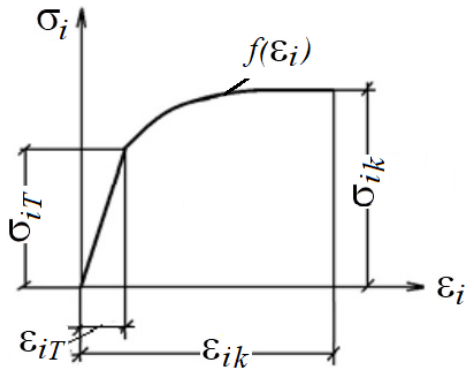

Fig. 2. Material strain diagram

To verify the convergence of the computational process based on the finite element used for different quantities, the problem was solved for elastic strain.

The function $\sigma_i = f(\varepsilon_i)$ is taken in the form of a parabola $\sigma_i = a_1\varepsilon_i^2 + b_1\varepsilon_i + c_1$ with numerical values of the constants: a = -6612835.5282 MPa; b = 242231.47902 MPa; c = 1795.0330258 MPa.

To verify the convergence of the computational process based on the finite element used for different quantities, the problem was solved for elastic strain.

The numerical values of normal stresses at internal pressure q = 8 MPa (elastic strain) in the initial section (S = 0.0) and the end section of the elliptical shell are given in Table 1 for various options for discretizing the structure along the meridional coordinate S (number of nodes NM) and along shell wall thickness h (number of nodes NT). Table 1 shows the normal stresses of the internal and external fibers.

Table 1. Values of normal stresses of the internal and external fibers, where σ_{11}^{in}, σ_{11}^{ex} are the meridional stresses of the internal and external fibers and σ_{22}^{in}, σ_{22}^{ex} are the circumferential stresses in internal and external fibers

NM × NT	Stresses, MPa							
	σ_{11}^{in}	σ_{22}^{in}	σ_{11}^{ex}	σ_{22}^{ex}	σ_{11}^{in}	σ_{22}^{in}	σ_{11}^{ex}	σ_{22}^{ex}
20×3	32.18	65.97	34.06	60.61	2.05	62.65	1.08	46.90
40×5	32.08	65.86	34.22	60.60	0.64	62.43	0.367	47.12
80×7	32.05	65.83	34.28	66.60	0.18	62.36	0.113	47.15
	S = 0.0				S = 16.06 cm			

Table 1 shows the values of physical stresses obtained using Hooke's law (2). Analysis of the results given in Table 1 indicates the convergence of the computational process and emphasizes the tendency towards zero meridional stresses in the end section (S = 16.06 cm).

Example 2. The structure shown in example 1 was loaded with pressure q = 45.6 MPa for a different number of steps (n_s = 10, 20, 40, 80). The calculation results based on Eqs. (15) and (19) turned out to be almost identical.

Meridional and circumferential stresses in internal (σ_{11}^{in}, σ_{22}^{in}) and external fibers (σ_{11}^{ex}, σ_{22}^{ex}) of the support section, as well as stress intensity (σ_i^{in}, σ_i^{ex}) based on Eq. (19) are given in Table 2.

Table 2. Values of meridional and circumferential stresses in the internal and external fibers of the support section, and stress intensity

n_s	Stresses, MPa					
	σ_{11}^{in}	σ_{22}^{in}	σ_i^{in}	σ_i^{ex}	σ_{22}^{ex}	σ_i^{ex}
10	158.19	340.19	319.18	249.67	418.11	355.56
20	160.97	343.45	327.56	215.71	367.71	310.98
40	161.22	343.77	333.43	223.05	380.12	327.36
80	162.36	345.88	336.72	216.65	369.98	319.58

Analysis of the results of Table 2 indicates the convergence of the computational process with an increase in the number of loading steps.

Meridional and circumferential stresses along the thickness of the shell support section are given in Table 3 under the load q = 45.6 MPa and n_s = 40.

Table 3. Values of meridional and circumferential stresses along the thickness of the shell support section

σ_{11}, MPa	161.22	170.99	178.54	187.85	196.65	205.61	223.05
σ_{22}, MPa	343.77	349.08	352.42	356.99	362.09	365.82	380.12

Diagrams of meridional (σ_{11}^{in}) and circumferential (σ_{22}^{in}) stresses are presented in Figs. 3 and 4 respectively. Numerical values of circumferential stresses shown in Fig. 4 are in adequate agreement with the numerical values of meridional stresses.

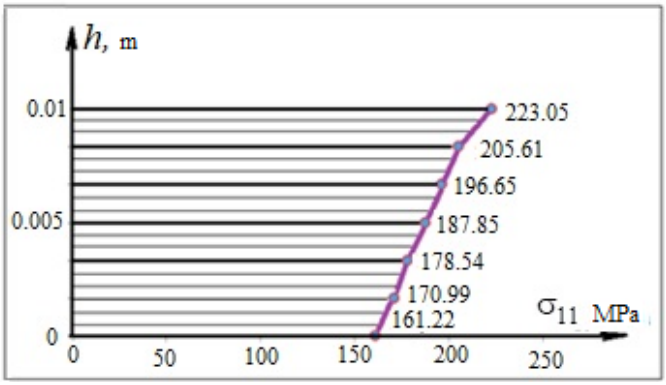

Fig. 3. Diagram of meridional stresses σ_{11} along the height of the support section

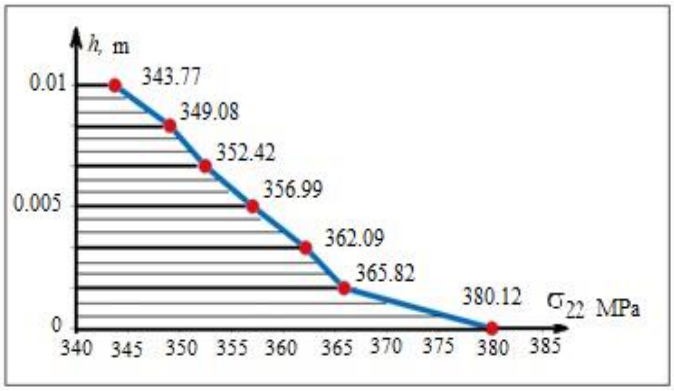

Fig. 4. Diagram of circumferential stresses σ_{22} of the support section

Table 4. Values of meridional and circumferential stresses in the internal and external fibers along the length of the meridian arc

Stresses, MPa	Length of meridian *S*, m												
	0.00	1.16	3.38	5.19	7.03	10.98	12.06	13.22	13.72	14.24	14.79	15.4	16.06
σ_{11}^{in}	161.22	160.29	161.09	159.08	156.27	144.30	135.55	117.86	106.79	91.31	70.62	41.28	-0.014
σ_{22}^{in}	343.77	341.67	339.76	331.62	319.41	290.67	284.24	280.08	280.17	277.79	276.19	275.29	274.25
σ_{i}^{in}	333.43	331.39	329.36	322.28	312.00	286.34	280.74	276.52	277.12	275.95	277.01	282.28	294.63
σ_{11}^{ex}	223.05	219.91	207.46	192.69	172.94	110.58	88.83	67.77	58.64	51.57	42.361	29.10	1.365
σ_{22}^{ex}	380.12	377.38	362.98	363.61	346.49	293.49	287.99	274.81	275.65	270.61	275.55	275.38	274.31
σ_{i}^{ex}	327.36	324.53	311.09	310.69	296.18	252.12	251.61	243.90	247.64	245.02	253.12	258.15	269.64

Table 4 shows the values of meridional and circumferential stresses, as well as stress intensities along the length of the meridian, in the internal and external fibers of the shell.

Based on the results of Table 4, graphs of meridional σ_{11}, circumferential σ_{22} and stress intensity σ_i were constructed (Fig. 5).

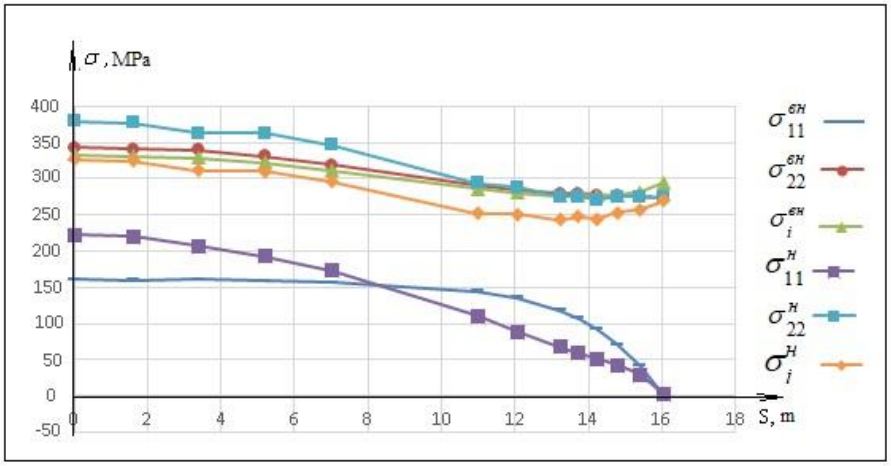

Fig. 5. Graphs of changes in meridional and circumferential stresses in fibers along the length of the meridian arc

From the values of stress intensities in the internal and external fibers on Fig. 5, it is clear that under conditions of plastic strain the material is near the surfaces. And since the meridional (σ_{11}) and circumferential (σ_{22}) stresses are tensile, it means that the material between the surfaces is under conditions of plastic strain. There are no areas of elastic strain at q = 45.6 MPa along the section thickness.

Based on Fig. 3 for meridional stresses, a static check of the equilibrium condition of the structure was performed (Fig. 1) $\sum \mathrm{x} = Q_q - Q_\sigma = 0$, where Q_σ is a stress endeavor; Q_q is a pressure endeavor q.

The error is $\delta = 0.6$ %. From the values of stress intensities in the internal and external fibers in Fig. 5, it can be seen that the entire body of the shell is under conditions of plastic strain $\sigma_i > \sigma_{iT}$ = 200 MPa along the entire thickness.

Conclusions

In the second variant of the physical equations (Eq. (14)) the following relations are accepted $P_{\Delta\varepsilon} = P^e_{\Delta\varepsilon} + P^p_{\Delta\varepsilon} = \frac{1-2\nu}{E} + 0$, in other words, it is assumed that during elastoplastic deformation ($\sigma_i > \sigma_{iT}$) the first invariant of the strain increment tensor changes according to the law of elastic deformation.

In the third variant of the defining equations (Eq. (18)) the relations $P_{\Delta\varepsilon} = P^e_{\Delta\varepsilon} + P^p_{\Delta\varepsilon} = \phi P_{\Delta\sigma}$ are used, which can be accepted either on the basis of experiment or on the basis of some hypothesis. In the first and second variants of the defining equations, the value $P^p_{\Delta\varepsilon} = 0$, and the value $P^p_{\Delta\varepsilon} = \frac{1-2\nu}{E}$ is used in the increments of elastic deformation throughout the entire process of elasto-plastic deformation.

In this work, in order to compare the variants of the defining equations, the expression $P_{\Delta\varepsilon} = P^e_{\Delta\varepsilon} + P^p_{\Delta\varepsilon} = \frac{1-2\nu}{E}$, is used, in which the results of the calculation of the presented example based on the second and third variants of the physical equations turned out to be almost identical.

When calculating structures for which the material dependence $P_{\Delta\varepsilon} = \phi P_{\Delta\sigma}$ is not linear, the third variant of physical equations should be used.

References

1. Malinin MM. *Applied Theory of Plasticity and Creep*. Moscow: Mashinostroenie Publ.; 1975. (In-Russian)
2. Golovanov AI, Sultanov LU. *Mathematical models of computational nonlinear mechanics of deformable media*. Kazan: Kazan State University; 2009. (In-Russian)
3. Petrov VV. *Nonlinear Incremental Structural Mechanics*. Moscow: Infra-Inzheneriya Publ.; 2014. (In-Russian)
4. Levin VA. *Nonlinear Computational Mechanics of Strength, Vol. 1: Models and methods. Formation and development of defects*. Moscow: Fizmatlit Publ.; 2015. (In-Russian)
5. Sedov LI. *Continuum Mechanics*. Moscow: Nauka Publ.; 1976. (In-Russian)
6. Samul VI. *Fundamentals of the theory of elasticity and plasticity*. Moscow: Vysshaya shkola Publ.; 1982. (In-Russian)
7. Demidov SP. *Theory of elasticity*. Moscow: Vysshaya shkola Publ.; 1979. (In-Russian)
8. Galimov KZ, Paimushin VN, Teregulov IG. *Foundations of the nonlinear theory of shells*. Kazan: Fan Publ.; 1996. (In-Russian)
9. Krivoshapko SN. On opportunity of shell structures in modern architecture and building. *Structural Mechanics of Engineering Constructions and Buildings*. 2013;1: 51–56. (In-Russian)
10. Reissner E. Linear and Nonlinear Theory of Shells. *Thin-Shell Structures: Theory, Experiment and Design*. New Jersey: Prentice Hall; 1974.
11. Levin VA, Vershinin AV. *Nonlinear Computational Mechanics of Strength, Vol. 2: Numerical methods. Parallel computing on a computer*. Moscow: Fizmatlit Publ.; 2015. (In-Russian)
12. Aldakheel F, Wriggers P, Miehe C. A modified Gurson-type plasticity model at finite strains: Formulation, numerical analysis and phase-field coupling. *Computational Mechanics*. 2018;62, 815–833.
13. Aldakheel F, Miehe C. Coupled thermomechanical response of gradient plasticity. *International Journal of Plasticity*. 2017;91: 1–24.
14. Aldakheel F. Micromorphic approach for gradient-extended thermo-elastic-plastic solids in the logarithmic strain space. *Continuum Mechanics Thermodynamics*. 2017;29: 1207–1217.
15. Sultanov LU. Analysis of finite elasto-plastic strains. Medium kinematics and constitutive equations. *Lobachevskii Journal of Mathematics*. 2016;37: 787–793.
16. Bathe KJ. *Finite element procedures*. New Jersey: Prentice Hall; 1996.
17. Golovanov AI, Tyuleneva ON, Shigabutdinov AF. *Finite element method in statics and dynamics of thin-walled structures*. Moscow: Fizmatlit Publ.; 2006. (In-Russian)
18. Wriggers P, Hudobivnik B. A low order virtual element formulation for finite elasto-plastic deformations. *Computer Methods in Applied Mechanics and Engineering*. 2017;327: 459–477.

19. Da Veiga LB, Lovadina C, Mora D. A Virtual Element Method for elastic and inelastic problems on polytope meshes. *Computer Methods in Applied Mechanics and Engineering*. 2017;295: 327–346.
20. Tutyshkin ND, Zapara MA. Constitutive relations of the tensor theory of plastic damageability of metals. In: *Problemy prochnosti, plastichnosti i ustojchivosti v mekhanike deformiruemogo tverdogo tela: Materialy VII mezhdunarodnogo nauchnogo simpoziuma, Tver', 16-17 dekabrya 2010 goda*. Tver: TvGTU Publ.. 2011. p.216–219. (In-Russian)
21. Il'ushin AA. *Plasticity: Elasto-plastic deformation*. St.-Peterburg: Lenand Publ.; 2018. (In-Russian)
22. Dzhabrailov ASh, Nikolaev AP, Klochkov YuV, Gureyeva NA. Finite element algorithm for implementing variants of physically nonlinear defining equations in the calculation of an ellipsoidal shell. *Materials Physics and Mechanics*. 2022;50(2): 319–330.
23. Dzhabrailov ASh, Nikolaev AP, Klochkov YuV, Gureyeva NA, Ishchanov TR. Calculation of an Elliptic Cylindrical Shell Outside Elastic Limits Based on the FEM with Various Forms of Defining Equations. *Journal of Machinery Manufacture and Reliability*. 2020;49: 518–529.
24. Gureeva NA, Kiseleva RZ, Nikolaev AP. Nonlinear deformation of a solid body on the basis of flow theory and realization of FEM in mixed formulation. *IOP Conference Series: Materials Science and Engineering*. 2019:675: 012059.
25. Gureeva NA, Klochkov YuV, Nikolaev AP, Yushkin VN. Stress-strain state of shell of revolution analysis by using various formulations of three-dimensional finite elements. *Structural Mechanics of Engineering Constructions and Buildings*. 2020;16(5): 361–379.
26. Magisano D, Leonetti L, Garcea G. Advantages of the mixed format in geometrically nonlinear analysis of beams and shells using solid finite elements. *International Journal for Numerical Methods Engineering*. 2016:109(9): 1237–1262.
27. Liguori F, Madeo A, Garcea G. A mixed finite-element formulation for the elasto-plastic analysis of shell structures. *Theoretical and Applied Mechanics*. 2023;26: 227–232.
28. Leonetti L, Le CV. Plastic collapse analysis of Mindlin–Reissner plates using a composite mixed finite element. *International Journal for Numerical Methods in Engineering*. 2016;105: 915–935.
29. Magisano D, Garcea G. Fiber-based shakedown analysis of three-dimensional frames under multiple load combinations: Mixed finite elements and incremental-iterative solution. *International Journal for Numerical Methods in Engineering*. 2020;121: 3743–3767.
30. Klochkov YuV, Pshenichkina VA, Nikolaev AP, Vakhnina OV, Klochkov MYu. Stress-strain state of elastic shell based on mixed finite element. *Magazine of Civil Engineering*. 2023;4(120): 12003.

About Author

Rumia Z. Kiseleva Sc
Candidate of Technical Sciences
Associate Professor (Volgograd State Agrarian University, Volgograd, Russia)

Natalya A. Kirsanova
Doctor of Physical and Mathematical Sciences
Associate Professor (Financial University under the Government of the Russian Federation, Moscow, Russia)

Anatoliy P. Nikolaev Sc
Doctor of Technical Sciences
Associate Professor (Volgograd State Agrarian University, Volgograd, Russia)

Yuriy V. Klochkov Sc
Doctor of Technical Sciences, Professor
Head of the Laboratory for Higher Mathematics (Volgograd State Agrarian University, Volgograd, Russia)

Yushkin V.N. Sc
Candidate of Technical Sciences
Associate Professor (Volgograd State Agrarian University, Volgograd, Russia)